Micro EDM Milling with Electrochemical Fabrication of Ultra-thin Microtools and Mapping of Electrical Microdischarges

M Cabrera, R Dahmani, Y Layouni, V Semet

Available online at www.sciencedirect.com

ScienceDirect

Procedia CIRP 42 (2016) 650 – 655

www.elsevier.com/locate/procedia

18th CIRP Conference on Electro Physical and Chemical Machining (ISEM XVIII)

Micro EDM milling with electrochemical fabrication of ultra-thin microtools and mapping of electrical microdischarges

M. Cabrera[a,]*, R. Dahmani[a], Y.Layouni[a], V. Semet[a]

Université de Lyon, Institut des Nanotechnologies de Lyon, UMR 5270 CNRS INSA ECL UCB CPE, Bâtiment Brillouin, 43 boulevard du 11 novembre 1918, F69622 Villeurbanne, France

* Corresponding author. Tel.: +33 4 72 73 14 33. *E-mail address:* michel.cabrera@univ-lyon1.fr

Abstract

The aim of this paper is to describe some possibilities allowed by a micro EDM milling machine, which has been entirely developed in our laboratory. Among other features, this machine does not make use of WEDG for fabricating the microtools. Instead of this, a compact low cost electrochemical reactor allows automated etching of tungsten microtools with a diameter ranging from 1 to 30 µm and very high aspect ratio (50-100). Thus, fragile microtools are obtained and regenerated without any intervention by the operator. Micro EDM milling is performed with such microtools thanks to a specially designed electronics based on a parallel architecture with 3 microcontrollers. The electrical signals of the micro discharges are continuously characterized which allow mapping of micro electrical discharges and contacts. It is demonstrated that the spatial distributions of discharges and contacts give valuable information on the micro EDM milling process. During the machining of microchannels in stainless steel, it is reported that the positions of contacts match with a low number of discharges. So, high tool wear and low part removal rate are related to a high number of contacts. Heterogeneous machining along the vertical Z axis and the horizontal XY axis can be also characterized.

Peer-review under responsibility of the organizing committee of 18th CIRP Conference on Electro Physical and Chemical Machining (ISEM XVIII)

Keywords: micro EDM milling; electrochemical etching; microtool; characterization of discharges; mapping of discharges

1. Introduction

The development of Micro Electrical Discharge Machining (EDM) is hindered by the lack of equipment suitable for basic research. As recognized in the literature, scientists have little access to the physical meaning of the parameters of commercial machines [1]. Therefore, our laboratory has been involved for several years in the development of a micro EDM milling machine allowing full control of all parameters.

The aim of this paper is to describe the possibilities allowed by our second generation machine. Among other features, this machine does not make use of Wire Electrical Discharge Grinding (WEDG) for fabricating the microtools. Instead of this, a compact low cost electrochemical reactor allows automated etching of tungsten microtools.

Machining is performed with such microtools thanks to an electronics based on a parallel architecture, which is reported below. The electrical signals of the micro discharges are continuously characterized during machining. This method avoids the limitations of the other methods reported in the literature which are based either on electrical measurement with digital oscilloscopes [2,3] or on indirect methods such as acoustic emission [4]. The proposed solution allows creating the map of the discharges and contacts between the tool and the part, which gives valuable information on the micro EDM milling process as demonstrated below.

2. Experimental set up

The principle of the machine and the experimental set up are shown respectively in Fig.1 and Fig. 2a. The machine is composed of:

Peer-review under responsibility of the organizing committee of 18th CIRP Conference on Electro Physical and Chemical Machining (ISEM XVIII)
doi:10.1016/j.procir.2016.02.296

- A first recipient (Fig. 2b) where a tungsten rod is electrochemically etched in order to fabricate the microtool.
- A second recipient (Fig. 2c) where this microtool is used to machine a part by micro EDM milling with a dielectric (deionised water in this article).

When the microtool is worn, it is returned to the first recipient and electrochemically cut. A stick slip actuator (not described below) allows pushing the rod so to renew the working length. Thus, fragile microtools are obtained and regenerated without any intervention by the operator.

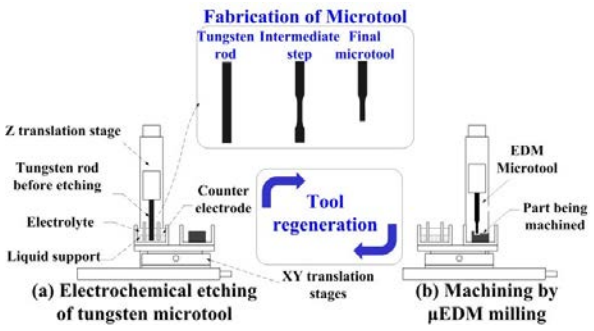

Fig. 1. Principle of the machine.

The machine is equipped with translation stages with stepper motors (0.3125 µm microstep), which allows moving the part to machine (316 L stainless steel in this article) and the microtool respectively in the horizontal XY and vertical Z directions. The gap between the tool and the part is adjusted with a piezoelectric actuator (90 µm range; 1.8 nm resolution). Two cameras with long distance zoom allow viewing the part and the micro tool (top and side views). All components are installed on a vibration isolation workstation.

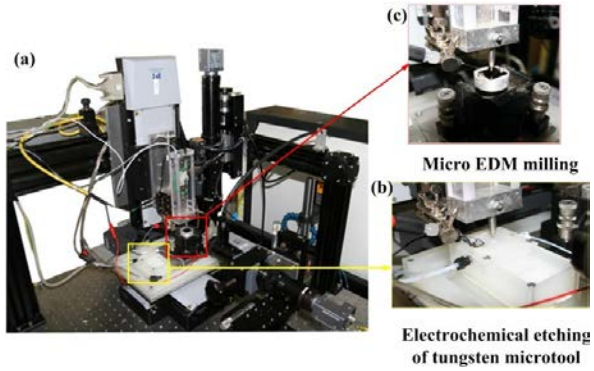

Fig. 2. Experimental set up.

3. Electrochemical fabrication of microtool

This process will be summarized below as it has been already described in [5]. The tungsten rod is immersed in the recipient containing the electrolyte (5Mol/L NaOH) on top of a non-conducting supporting dielectric liquid (non-mixable with the electrolyte). A pulsed current is applied between the rod and a platinum counter electrode with appropriate time of application T_{ON} (with alternate polarities T^+/T^-) and rest time T_{OFF} (Fig. 3).

The electrochemical dissolution of tungsten is then started. The lower part of the rod (in the dielectric) is unchanged during the process whilst the intermediate part (in the electrolyte) is made thinner. The resulting shape resembles a dumb-bell.

Then the rod is translated upward in order to cut off the lower part of the dumb-bell.

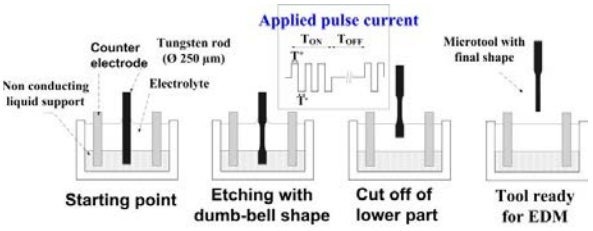

Fig. 3. Electrochemical fabrication of ultra-thin microtools.

Starting with a diameter of 250 µm, the rod is progressively made thinner with a final diameter typically ranging from 3 to 30 µm with F_f 50-100 aspect ratio (Fig. 4). With such thin microtools, one difficulty is to avoid damaging during EDM machining in the event of a mechanical contact with the part. This relies on the detection of a possible contact with electronics means described below and the immediate retraction of the microtool (see also [6] for detailed examples of micro EDM machining with Ø 9 µm microtool).

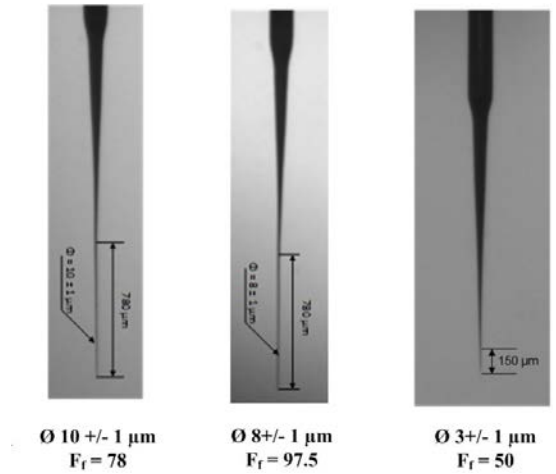

Fig. 4. Ultrathin microtools (CCD camera with Navitar x12 zoom).

4. Electronics of the machine

The electronics of the machine (Fig. 5) is based on a parallel architecture with three low cost ATMega162 microcontrollers (µC). This solution allows detecting events which may happen simultaneously in the gap region in order

to treat them independently. A PC with LabView software is in charge of the interface between the operator and the machine.

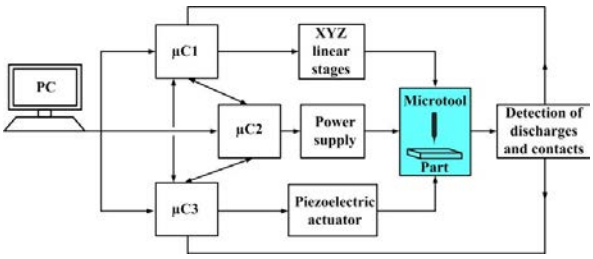

Fig. 5. Electronics of the machine with three microcontrollers.

The electric generator is of RC type (Fig. 6). A ballast resistor R_b in series with the microtool may be used to reduce the energy of discharges as reported in [6]. However, in this paper for simplicity, there is no ballast resistor ($R_b = 0\ \Omega$).

The difference in electric potential between the part and the microtool is reduced by a divider and continuously characterized with a series of three comparators with adjustable threshold, which outputs are connected to the counters of the µCs (Fig. 6).

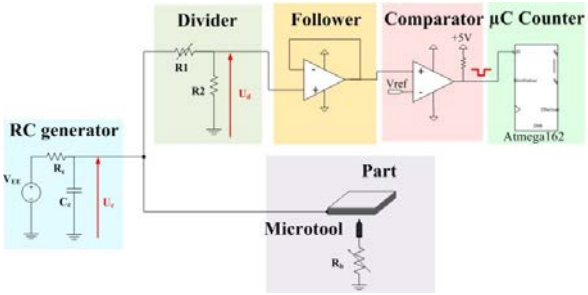

Fig. 6. Electronics for the detection of discharges and contacts.

As shown in Fig. 7, three thresholds can be set independently to detect high power discharges (large voltage drops across the working capacitance C_C), low power discharges (small voltage drops) and possible contacts between the tool and the part which may damage the tool.

Referring to Fig. 5, µC1 is in charge of the movements of the XYZ linear stages and can also detect discharges and contacts.

In case of contact between the part and a microtool of diameter below 20-30 µm, the difference of potential is determined by the apparent contact area [7] and the presence of dielectric. Thus it is not 0 V. Therefore, the threshold is set above 0 V and the contact should last at least during 20 µs in order to be taken into account by the µCs. In such a case, the movement of the machine is stopped and the microtool is moved up and down of 30 microsteps in order to remove the contact and pursue machining.

During the entire machining process, µC1 knows the relative position of the tool and the part when a discharge or a contact happens. The solution proposed here does not suffer from the limitations described in the literature which consist in sampling the process during limited time frame [2,3]. Thus, fast and rare events (for example 100 ns discharges), which may happen at any time during a process which may last for hours, are taken into account.

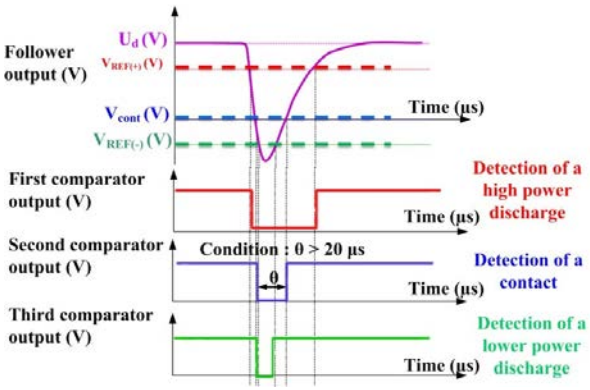

Fig. 7. Detection and counting of discharges and contacts.

Mapping of electrical discharges and contacts

4.1. Principle of experiment

The goal of this section is to demonstrate that the spatial distributions of discharges and contacts give valuable information on the micro EDM milling process.

A series of 6 microchannels is machined in polished 316L stainless steel at increasing target depths H_c from 50 to 300 µm (Fig. 8). The channel length is 500 µm. The microtool diameter is 25 µm and the initial gap is 5 µm +/- 1 µm.

The movement of the microtool is described below. Back and forth movements are performed along the Y axis at constant speed 312 µm/s. Then the microtool comes back to the initial Y position and it moves down along the Z axis of 1 microstep (0.3125 µm).

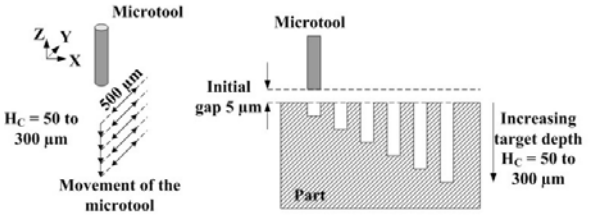

Fig. 8. Movement of the microtool for the machining of microchannel at increasing target depth H_c 50, 100, 150, 200, 250 and 300 µm.

The power supply is switched on at the beginning of the process and switched off only at the end. The operating voltage V_{EE} is 50 V and the working capacitance C_C and resistor R_C are respectively 4.7 nF and 100 Ω.

The threshold levels $V_{REF(-)}$,V_{cont} and $V_{REF(+)}$ for the detection of high energy discharges, contacts and low energy discharges are respectively set at -0.1 V, 1.4 V and +0.1 V with 1/29 attenuation at the divider (Fig. 7).

The gap regulation with µC3 (Fig. 5) is inactivated but the microtool is put in oscillation with the piezoelectric actuator at 100 Hz with 9 µm amplitude; the lowest point being at initial gap value. This is used to help flushing the gap with deionized water (note that the microtool is not rotated during micro EDM machining).

Fig. 9a and Fig. 9b show the microchannels as observed from the top with the CCD camera of the machine.

The machined microchannels are molded with polydimethylsiloxane (PDMS) is order to facilitate characterization. The result can be seen in Fig. 9c which shows a lateral view of the parts and their images reflected by the stainless substrate (the dotted line represents the estimated position of the substrate).

The width (W) and height (H) of the molded parts are reported in Fig. 9d (as measured with an optical microscope). For example for a target depth of 300 µm, the measured depth of the channel is 210 µm and its width is 61 µm.

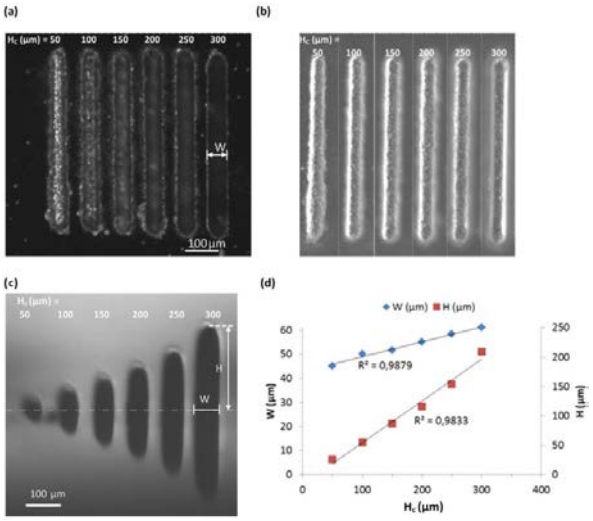

Fig. 9. (a) Top view of the machined microchannels with focus on the upper part; (b) Top view of the machined microchannels with focus on the lower part; (c) Side view of the microchannels molded with PDMS; (d) Height (H) and width (W) of PDMS parts at different target heights H_C.

Interestingly, Fig. 10a is a view of the microtool in front of the part without water in the gap and before machining (lateral view with CCD camera of the machine). It shows the initial gap of 5 µm.

Fig. 10b to Fig. 10g show the tool after each the machining of each channel. The same tool is used for all channels but the initial gap is set up each time so that the wear length of the tool can be estimated from this picture.

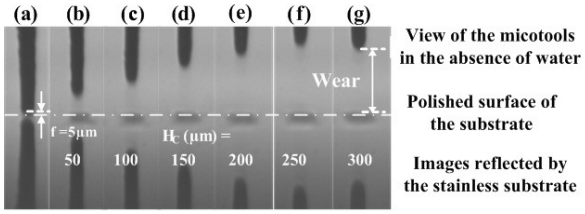

Fig. 10. (a) Microtool at initial gap; (b) to (g) Microtool wear after machining.

The machining is characterized in terms of (Table 1):

- Material removal rate (MRR) which is the ratio of the volume removed from the part with machining time (µm^3/min).
- Tool removal rate (TRR), which is the ratio of the wear volume of the tool with machining time (µm^3/min).
- Relative tool wear RTW which is the ratio of TRR with MRR (%).

The conclusion is that the MRR increases with target depth and the TRR decreases. In other words, in this experiment, the wear of the tool is reduced and the machining is more efficient when the target depth increases.

Table 1. Material removal rate, tool removal rate, relative tool wear at different values of target depth

Target depth H_C (µm)	MRR (µm^3/min)	TRR (µm^3/min)	RTW (%)
50	6.6E+04	9.2E+02	1.40
100	8.0E+04	8.3E+02	1.03
150	8.7E+04	7.8E+02	0.91
200	9.3E+04	7.8E+02	0.84
250	1.0E+05	7.1E+02	0.68
300	1.2E+05	5.5E+02	0.44

In other respects, Fig. 11 shows the number of discharges and contacts versus the target machining depth. For simplicity, the number of high power energy discharges was added to the number of low power energy discharges. As expected the number of discharges grows when more material is removed, that is to say when the target depth increases, but very surprisingly the number of contacts does not.

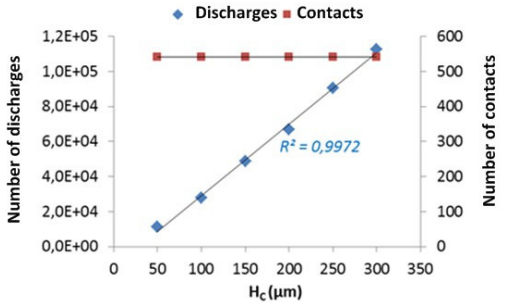

Fig. 11. Number of discharges and contacts for different machining depth H_C.

4.2. Detailed analysis of the microchannel with 300 µm target depth

In order to better understand this point, the positions of discharges and contacts have been collected during machining of the microchannel at 300 µm target depth.

As a result, Fig. 12 shows the contacts as function of the position input commands Y and Z of the translation stages (The real Y value of the part is close to the Y position input command, but the Z real value of the tool is different of the Z position input command because of the tool wear). Every black point represents a contact.

73% of the contacts are detected at both ends of the microchannels along Y and in the top 50 µm layers along Z.

The contacts at the ends may be caused by the vibrations of the microtool during back and forth movements and may be reduced with further machine optimization. Therefore, we shall not discuss this point below.

The interesting point here is the difference of performance in machining near the surface and in the core of the substrate.

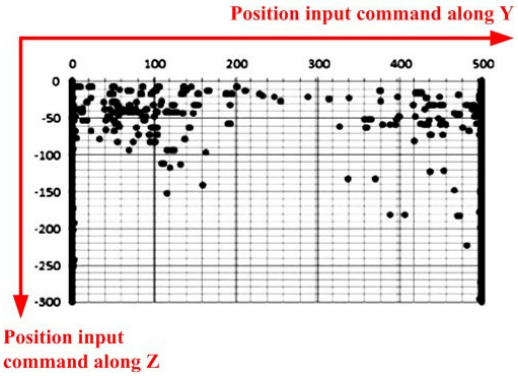

Fig. 12. Mapping of contacts as function of the YZ position input commands during the machining of the microchannel (Y = 0 to Y = 500 µm and Z = 0 to Z = H_C = 300 µm).

In Fig. 13, the discharges have been superimposed to the contacts. Every black point represents a contact as previously reported but this time, every colored pixel represents the number of discharges detected in 5x5 µm² (sum of high power and low power discharges).

The number of discharges is higher at deeper machining depth. The regions where the number of discharges is low (blue points) match with the regions where the number of contacts is high (black points). Furthermore, when the removal of material is efficient as depicted with a high number of discharges (red points), the number of contacts is low.

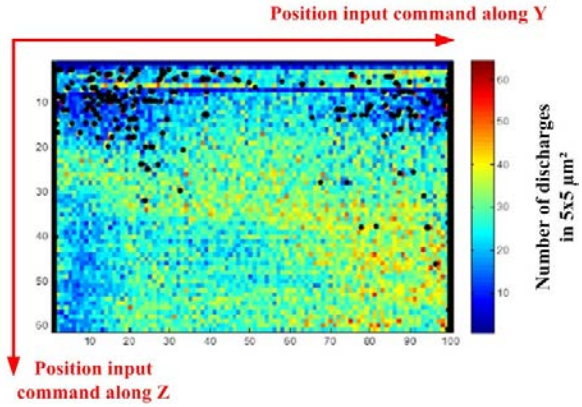

Fig. 13. Mapping of contacts (black points) and discharges (coloured pixel) during the machining of the microchannel (Y = 0 to Y = 500 µm and Z = 0 to Z = H_C = 300 µm).

4.3. Mapping of discharges and contacts of all microchannels

A similar analysis has been performed for all microchannels with consistent results. Fig. 14 shows the superimposition of the number of contacts and discharges at increased target depth. Most contacts are located at both ends of microchannel and in the first 50 µm top layers in regions with a low number of discharges.

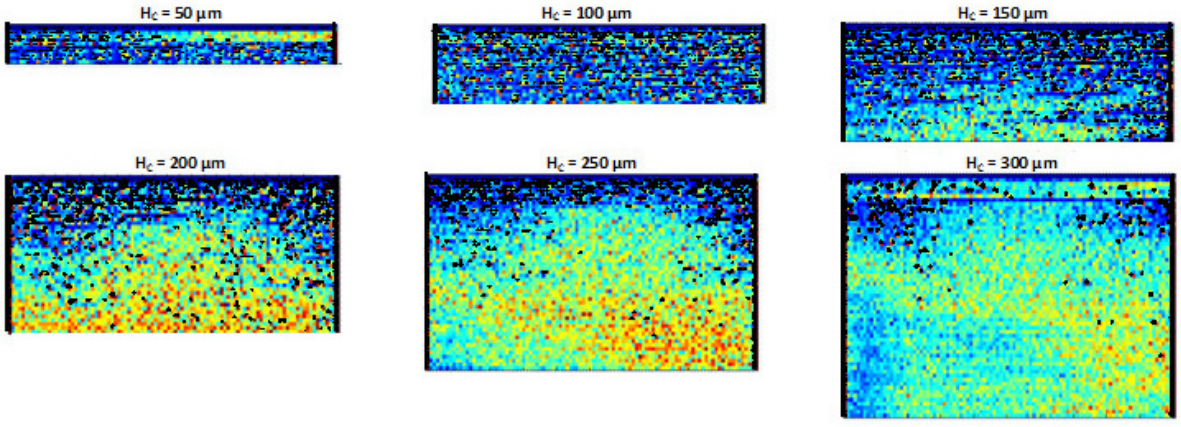

Fig. 14. Mapping of contacts (black points) and discharges (colored pixel) during the machining of microchannel at different target machining depth (Y = 0 to Y = 500 µm and Z = 0 to Z = H_C). Same axis and axis than Fig. 13. The scale of the pixel is 5x5 µm².

5. Conclusion

This result explains why, in this experiment, the number of contacts is relatively constant and does not vary at increased target depth. Indeed most contacts happen in the 50 µm top layers. So the number of contacts does not depend on the target depth provided that this one is sufficient.

It is known from the literature that the tool wear depends on the discharge energy. If we suppose that it depends also on the number of contacts, this may explain why machining is more efficient at increased target depth: the tool wear is important in the top layers and decrease significantly below (it is important to note that this result has been obtained with the gap regulation inactivated).

Further research will investigate the reasons for such heterogeneous machining along the Z axis. Different possibilities can be explored such as:

- The effect of polishing which may modify the metallurgy of the part near the surface.
- The mechanism of formation of the white layer.
- The mechanism of formation of the electrical discharges which may be easier inside the channel than at the top the part, etc.

However, our conclusion is that it has been demonstrated that the spatial distributions of discharges and contacts give valuable information on the micro EDM milling process.

Acknowledgements

This work was financed by the FUI ConProMi from the Region Rhône-Alpes and the EEC FEDER.

References

[1] Liu K, Lauwers B, Reynaerts D. Process capabilities of Micro-EDM and its applications. Int J Adv Manuf Tech 2010; 47:11-19.
[2] Bissacco G, Hansen HN, Tristo G, Valentincic J. (2011). Feasibility of wear compensation in micro EDM milling based on discharge counting and discharge population characterization. CIRP Annals-Manufacturing Technology 2010; 60(1):231-234.
[3] Ferri C, Ivanov A, Petrelli A. Electrical measurements in µ-EDM. J. Micromech. Microeng. 2008; 18(8):085007.
[4] Smith C, Kosh P. Applications of acoustic mapping in electrical discharge machining. CIRP Annals-Manufacturing Technology 2013; 62(1):171-174.
[5] Layouni Y, Girardin G, Benilov A, Semet V, Morin P, Cabrera M. Onboard Electrochemical Fabrication of Microelectrodes for Micro EDM Milling. Micro and Nanosystems 2011; 3(3):215-221.
[6] Dahmani R, Layouni Y, Semet V, Cabrera M. Micro EDM milling with low energy discharges and thin microtool. In: Annoni M, Fassi I, Wiens GJ, Dimov S, editors. Proceedings of the 4M/ICOMM2015 Conference. Research Publishing; 2015. p.50-53.
[7] Kogut L, Komvopoulos K. Electrical contact resistance theory for conductive rough surfaces. Journal of Applied Physics 2003; 94(5):3153-3162.